Metallophysics and Advanced Technologies
Металофіз. новітні технол.
Metallofiz. Noveishie Tekhnol.
2025, vol. 47, No. 9, pp. 973–982
https://doi.org/10.15407/mfint.47.09.0973
Reprints available directly from the publisher

PACS numbers: 06.60.Vz, 61.72.Ff, 62.20.mm, 62.20.Qp, 68.35.Gy, 81.20.Vj, 81.40.Pq

Performance of Double-Side Friction Stir Welded AA7075 Aluminium Alloy

V. Kiran Kumar[*,**], K. V. Durga Rajesh[*], S. R. Koteswara Rao[***], T. Srinivasa Rao[****]

[*]*Department of Mechanical Engineering,*
Koneru Lakshmaiah Education Foundation,
522 302 Vaddeswaram,
Andhra Pradesh, India
[**]*Department of Mechanical Engineering,*
Vasireddy Venkatadri Institute of Technology,
522 508 Nambur,
Guntur, Andhra Pradesh, India
[***]*Department of Mechanical Engineering,*
Sri Sivasubramaniya Nadar College of Engineering,
603 110 Chennai,
Tamil Nadu, India
[****]*Cornerstone Academy Private Limited,*
600 129 Chennai,
Tamil Nadu, India

Nowadays, the automotive industry is increasingly emphasizing lightweight structures to enhance fuel efficiency, vehicle performance and comply with emission regulations. Traditionally, reducing steel-sheet thickness and boosting strength has been the go-to method for weight reduction, but this approach often compromises panel stiffness. To address the same, there is a growing interest in replacing steel with lighter materials like aluminium, which offer comparable structural properties. AA7075, an aluminium 7000 series alloy with high strength, prepared with precipitation hardening, is one

Corresponding author: V. Kiran Kumar
E-mail: kiran.rlwc@gmail.com

Citation: V. Kiran Kumar, K. V. Durga Rajesh, S. R. Koteswara Rao, and T. Srinivasa Rao, Performance of Double-Side Friction Stir Welded AA7075 Aluminium Alloy, *Metallofiz. Noveishie Tekhnol.*, **47**, No. 9: 973–982 (2025), DOI: 10.15407/mfint.47.09.0973

alternative. However, it is regarded to be difficult to join 7075 plates by conventional fusion-welding methods. Friction stir welding, being a solid-state joining process, is proved as a viable technique to join successfully these high-strength alloys, in particular, AA7075. However, the friction stir welding causes reductions in weld properties, and the reduction is more pronounced in thick section welds. Double-side friction stir welding is considered as one of the possible solutions to address the problem of weld-property reductions. In the present study, 6.35 mm-thick AA7075-T651 plates are friction stir welded from both sides. Mechanical properties of the welded joints are evaluated using tensile tests as per ASTM B557 standards and hardness tests. Furthermore, the weld microstructures are also examined using optical microscopy. Higher hardness values occur in weld nugget, and the heat-affected zone records lower hardness values. The weld zone has exhibited joint efficiency of 67% in terms of yield strength, and the tensile fractures are found to take place in the weld nugget. Weld nugget region of friction stir weld exhibits fine equiaxed, recrystallized grains, while heat-affected zone is seen with marginal grain growth.

Key words: double-side friction stir welding, aluminium alloy 7075, weld microstructure, tensile properties, hardness survey.

Автомобільна промисловість сьогодні все більше потребує легких конструкцій для підвищення ефективности використання палива, продуктивности автомобілів і відповідности нормам викидів. Традиційно основним методом пониження ваги та підвищення міцности було зменшення товщини крицевого листа, але цей підхід часто понижує жорсткість панелей. Для вирішення цієї проблеми було запропоновано замінити криці легшими матеріялами, такими як алюміній, які демонструють порівнянні структурні властивості. AA7075, алюмінійовий стоп серії 7000 з високою міцністю, одержаний методом дисперсійного гартування, є однією з альтернатив. Однак вважається, що з'єднання пластин 7075 звичайними методами зварювання топленням є складним. Зварювання тертям з перемішуванням, що є процесом з'єднання у твердому стані, виявилося життєздатною технікою для успішного з'єднання цих високоміцних стопів, зокрема AA7075. Однак такий спосіб призводить до погіршення властивостей зварювання, і це пониження більш виражене у товстих зварних швах. Двостороннє зварювання тертям з перемішуванням вважається одним з можливих рішень для розв'язання проблеми пониження властивостей зварювання. У даній роботі пластини AA7075-T651 товщиною у 6,35 мм були зварені тертям з перемішуванням з обох боків. Механічні властивості зварних з'єднань оцінювали за допомогою випробувань на розтяг відповідно до стандартів ASTM B557 та випробувань на твердість. Окрім того, мікроструктуру зварного шва досліджували також за допомогою оптичної мікроскопії. Вищі значення твердости спостерігаються у місці зварювання, а зона термічного впливу має нижчі значення твердости. Зона зварювання продемонструвала ефективність з'єднання у 67% з точки зору межі плинности, і було виявлено, що в зварному шві відбуваються розривні руйнування. Область зварного шва, одержаного тертям з перемішуванням, має дрібні рівновісні, рекристалізовані зерна, тоді як у зоні термічного впливу

відбувається незначний ріст зерен.

Ключові слова: двостороннє зварювання тертям з перемішуванням, алюмінійовий стоп 7075, мікроструктура шва, властивості під час розриву, дослідження твердости.

(Received 17 April, 2025; in final version, 30 August, 2025)

1. INTRODUCTION

The 7xxx aluminium alloys stand out for their heat treatability and ability to offer the highest strengths among all aluminium alloys. Their remarkable strength-to-weight ratio and corrosion resistance have made them a staple in various aerospace and structural applications. However, joining these high-strength aluminium alloys using traditional fusion welding techniques presents challenges due to their high thermal conductivity, which often leads to weld defects such as porosity and solidification cracking. The dendrite structure formed during conventional welding also contributes to a significant reduction in mechanical properties [1–3].

Specifically, AA7075 sheet and plate products find extensive use in automotive industry where a balance of high strength, moderate toughness, and corrosion resistance is crucial. Aluminium and magnesium have densities of 2.7 $g \cdot cm^{-3}$ and 1.74 $g \cdot cm^{-3}$, respectively, significantly lower than steel (7.86 $g \cdot cm^{-3}$). However, aluminium can face availability issues for high-volume production. Therefore, a strategic blend of aluminium and magnesium, coupled with advanced joining techniques like friction stir welding, emerges as a promising solution for next-gen automobile applications. While these alloys are typically considered non-weldable using commercial processes and are often assembled using riveted construction, the advent of Friction Stir Welding (FSW) technology has provided a viable alternative, particularly, for welding high-strength aluminium alloys compared to traditional fusion techniques.

FSW is a solid-state, hot-shearing process well suited for joining nonferrous metals and alloys, offering notable advantages such as lower heat generation, absence of melting, reduced defects, and minimal distortion [4–8]. This process has gained traction in industries like automotive and aerospace for producing sound joints in high-strength aluminium alloys. However, improper welding parameters during FSW can lead to defects and compromise the mechanical properties of the joints [9].

During FSW, a non-consumable rotating cylindrical tool with a shoulder and threaded pin plunges into the butting surface of rigidly clamped plates placed on a backing plate. Welding occurs through friction-induced heat between the tool and plates, resulting in severe

plastic deformation and material flow as the tool moves along the welding direction. The weld consists of several zones, including the heat-affected zone (HAZ), thermomechanically affected zone (TMAZ), and dynamically recrystallized zone known as the weld nugget (WN). The fine grain structure in the centre of the weld region significantly influences the mechanical properties [10, 11].

Despite FSW effectiveness in joining high-strength alloys like AA7075, it can lead to reductions in weld properties, particularly noticeable in thicker welds [12, 13]. Double-side friction stir welding has emerged as a potential solution to mitigate these weld property reductions [14]. In the present study, 6.35 mm-thick AA7075-T651 plates were subjected to double-side friction stir welding, followed by a thorough evaluation of mechanical properties and examination of weld microstructures.

2. EXPERIMENTAL PROCEDURE

In the current study, 6.35 mm-thick plates of AA7075–T651 alloy were used, having a composition of Al–5.6% Zn, 2.5% Mg, 1.6% Cu, 0.23% Cr, and 0.08% Fe by weight. These plates were cut and machined into 110 mm-width and 200 mm-length coupons. To perform friction stir welding, an appropriate tool made of M2 grade tool steel with a tapper threaded pin profile was employed, featuring specific dimensions such as a 3.5 mm-pin length, 6 mm-pin major diameter, 3 mm-pin minor diameter, 15 mm-shoulder diameter, and a 1.5 mm pitch of threads, as illustrated in Fig. 1.

Through a series of rigorous trials, optimal welding parameters were determined to achieve flawless welds, including a pin rotational speed of 1000 rpm, a pin travel speed of 250 mm/min, and a 1.5° tilt angle between the FSW tool and the plates that are joined. Double-side friction stir welding (DS FSW) was performed sequentially on a vertical milling machine. The second pass (side 2) was welded after completing the first pass (side 1), with the advancing side (AS) of side 1 intentionally aligned to become the retreating side (RS) of side 2. The welded joints are presented in Fig. 2.

For microstructural analysis, advanced optical microscopy

Fig. 1. Image of the tool used for friction stir welding trials.

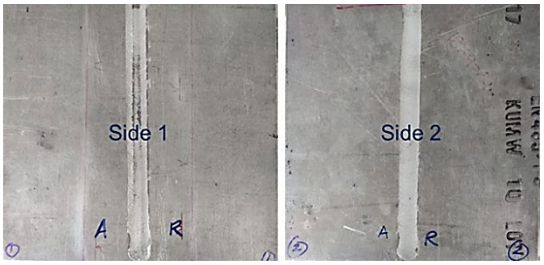

Fig. 2. Double side friction stir welded joint showing the weld region on both sides of the joint.

techniques were employed. Carefully prepared samples from the welds underwent a polishing process using various emery papers starting from 800 through 1200 grit size, culminating in final polishing using diamond compound (1 micron particle size) in a high-precision single disk polishing machine. These polished samples were then etched using standard Keller's reagent (comprising 5 ml HNO_3, 2 ml HF, 3 ml HCl, and 190 ml distilled water) to unveil the intricate microstructures within the welds. Fractured surfaces of tensile-tested specimens were also examined using scanning electron microscopy (SEM). Transmission electron microscopy (TEM) specimens were extracted from the parent metal and the weld nugget region of double-side friction stir weld using electrical discharge machining (EDM). Initial sample thinning was performed manually at low speeds to minimize thermal effects. Final thinning was achieved through electrolytic polishing using a solution of nitric acid in methanol. TEM studies were conducted using a JEM-2100 transmission electron microscope operating at 200 kV.

Transverse tensile specimens, in compliance to the stringent ASTM B557 standards, were meticulously prepared from the welds in their as-welded state. Room-temperature tensile tests were conducted using an advanced universal tensile testing machine. Hardness testing was carried out by Vickers microhardness tester. The readings were considered at the mid-thickness of the joint. Each indentation was taken with the spacing of 0.5 mm between adjacent measurements, at a load of 200 g and for a dwell time of 10 s each.

3. RESULTS AND DISCUSSION

3.1. Tensile Properties

The outcomes of the tensile tests are presented in Table 1. It is evident that friction stir welding led to a decrease in strength values compared to the unaltered base material. The yield strength, tensile strength and percent elongation values of the welded joint were found to be 360

MPa, 435 MPa and 7, respectively. The joint efficiency, calculated based on yield strength, was determined to be 67%. Moreover, each of the three weld samples experienced fracture at the weld nugget in a 45° shear mode, as depicted in Fig. 3. Fracture surface of the tensile tested samples is shown in Fig. 4. It was realized that tensile fractures occur in ductile mode as fine dimples can be observed.

TABLE 1. Results of transverse tensile testing (average of three tests).

Parameter	Base material	DS FS weld
Yield strength (0.2% proof) (MPa)	539	360
Ultimate tensile strength (MPa)	609	435
Elongation (%)	13	7
Joint efficiency in terms of YS (%)	–	67
Fracture location	–	WN

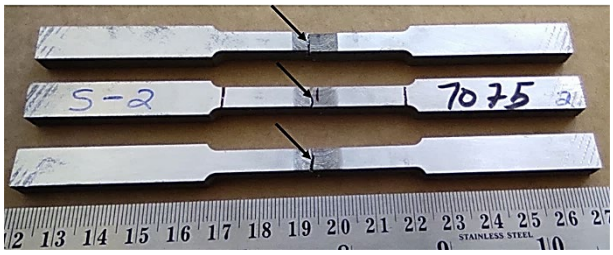

Fig. 3. Tensile fractures of double-side friction stir welded joint of AA7075 (arrowhead shows failure location).

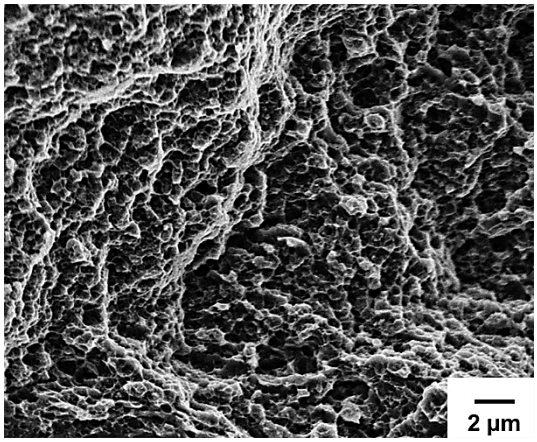

Fig. 4. SEM image exhibiting the fracture mode of the tensile-tested specimens.

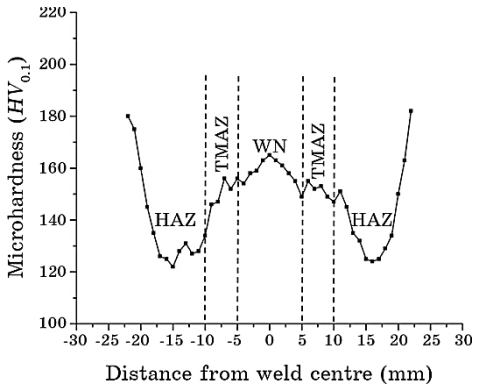

Fig. 5. Microhardness profile of the double-side friction stir welded joint.

3.2. Hardness Survey

Microhardness curve drawn from the readings obtained with 0.5 mm-spacing is presented in Fig. 5. As can be clearly seen, hardness profile was a typical 'W' shaped curve showing higher hardness in the weld nugget region and lower hardness in the heat-affected zone. The reduced grain size due to recrystallization of the material in the weld nugget could be the reason for higher hardness in the region. However, the high hardness could not show any effect on tensile strength of the material since all the tensile samples broke in the WN region itself. Increased hardness tackles the challenges associated with steel and contributes to further reducing vehicle weight.

3.3. Optical Microscopy

In Figure 6, the macrograph showcasing a double-side friction stir welded AA7075, highlighting a flawless weld with no discernible defects. The image clearly delineates various distinct weld zones such as the WN, the TMAZ, and the HAZ.

Figure 7 represents the micrographs depicting the parent material and the corresponding weld zones. Figure 7, *a* unveils the microstructure of parent metal, characterized by large elongated pancake-shaped grains, indicative of a hot rolled structure. Contrarily, Fig. 7, *b* reveals the microstructure of weld nugget, showcasing a fine and equiaxed grain formation resulting from recrystallization. The recrystallized fine grain structure could be the reason for the higher hardness in the weld nugget as the same is typical in case of friction stir welded aluminium alloys. Figure 7, *c* provides insight into the thermo-mechanically-affected zone, displaying a highly deformed grain structure, a consequence of the thermal and

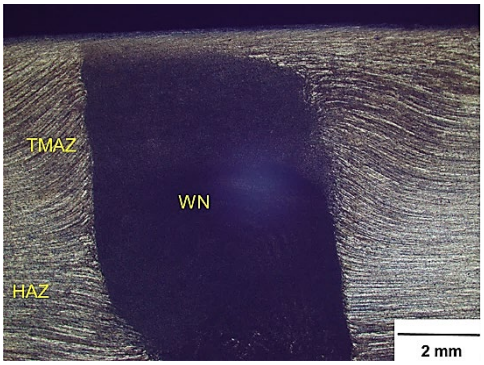

Fig. 6. Cross section of the weld showing various weld zones of double-side friction stir welded AA 7075.

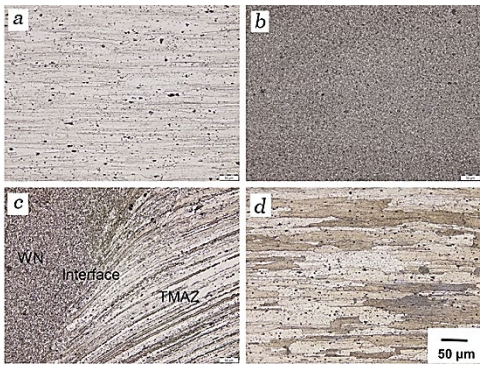

Fig. 7. Microstructures of the weld joint: *a*) parent metal; *b*) weld nugget; *c*) WN-TMAZ interface; *d*) HAZ.

mechanical effects of welding process. A defect free, clear interface zone of TMAZ and WN can also be seen in the same, which is an indication of solid weld joint between the parent work pieces. Finally, Fig. 7, *d* presents the heat-affected zone micrograph, which mirrors the grain structure of the parent metal, but with noticeable grain growth attributed to the heat input during welding.

3.4. Transmission Electron Microscopy

Figure 8 presents the characteristic precipitate morphology of AA7075 parent material in the T651 ageing condition and the weld nugget of the double side friction stir welded joint. As evident in Fig. 8, *a*, the parent metal contains two distinct types of strengthening precipitates, differentiated by size and morphology, consistent with

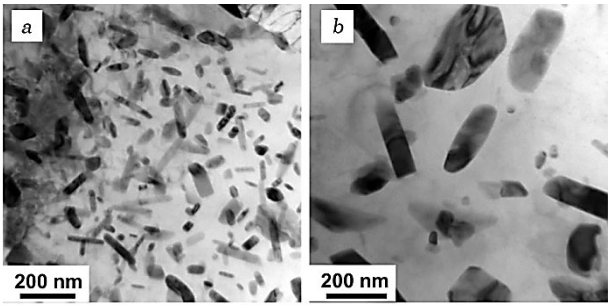

Fig. 8. Transmission electron microscopy images: *a*) parent metal; *b*) weld nugget.

prior reports by Wert [15] and Lorimer [16]. The first group comprises larger precipitates (50–80 nm), while the second consists of finer particles (20–25 nm). Wert [15] identified the larger precipitates as an isomorphous solid solution of $MgZn_2$ and MgAlCu, denoted as $Mg(Zn_2,AlCu)$. In contrast, Lorimer [16] characterized them as $Mg_{32}(Al,Zn)_{49}$ with a b.c.c. crystal structure. Thus, these precipitates may correspond to either phase. The presence of these strengthening precipitates, formed during deformation and T651 ageing, contributes to the base-material ultimate tensile strength of $\cong$600 MPa, *i.e.*, significantly higher than the $\cong$200 MPa observed in the annealed condition.

Figure 8, *b* presents the TEM micrograph of the weld nugget region in double-side friction stir welded joints. The welding thermal cycles, typically exceeding the solution temperature while remaining below the base-metal melting point, induced dissolution of strengthening precipitates in the weld nugget. However, TEM studies revealed partial re-precipitation and subsequent coarsening of some strengthening precipitate particles, attributable to favourable post-weld cooling rates. The dissolution and coarsening of strengthening precipitates could be considered responsible for tensile fractures in the weld nugget.

4. CONCLUSIONS

The conclusions drawn from the experiments on the FSW joint of AA7075 alloy samples are as follow.

1. AA7075 alloy 6.35 mm-thick plates can be successfully welded using friction stir welding from both sides.
2. The nugget region of the welded joint exhibited fine equiaxed recrystallized grains, while heat affected zone exhibited no change in grain structure excepting marginal grain growth.

3. Higher hardness values occurred in weld nugget and heat affected zone recorded lower hardness values.
4. The weld exhibited joint efficiency of 67% in terms of yield strength and the tensile fractures occurred in the weld nugget.

REFERENCES

1. M. B. D. Ellis and M. Strangwood, *Mater. Sci. Technol.*, **12**, Iss. 11: 970 (1996).
2. S. W. Williams, *Air Space Eur.*, 3: 64 (2001).
3. M. Ericsson and R. Sandstrom, *Int. J. Fatigue*, **25**: 1379 (2003).
4. T. Srinivasa Rao, G. Madhusudhan Reddy, and S. R. Koteswara Rao, *Trans. Nonferrous. Met. Soc. China*, **25**, No. 6: 1170 (2015).
5. T. Srinivasa Rao, G. Madhusudhan Reddy, G. Srinivasa Rao, and S. R. Koteswara Rao, *Int. J. Mater. Res.*, **105**, Iss. 4: 375 (2014).
6. K. Thamilarasan, S. Rajendraboopathy, G. Madhusudhan Reddy, T. Srinivasa Rao, and S. R. Koteswara Rao, *Mater. Test.*, **58**, Nos. 11–12: 932 (2016).
7. C. G. Rhodes, M. W. Mahoney, W. H. Bingel, R. A. Spurling, and C. C. Bampton, *Scr. Mater.*, **36**: 69 (1997).
8. M. W. Mahoney, C. G. Rhodes, J. G. Flintoff, R. A. Spurling, and W. H. Bingel, *Metall. Mater. Trans. A*, **29**: 1955 (1998).
9. R. S. Mishra and Z. Y. Ma, *Mater. Sci. Eng. R*, **50**, Iss. 1–2: 1 (2005).
10. T. Srinivasa Rao, G. Madhusudhan Reddy, and S. R. Koteswara Rao, *La Metall. Ital.*, **1**, No. 5: 29 (2016).
11. T. Srinivasa Rao, G. Madhusudhan Reddy, and S. R. Koteswara Rao, *Mater. Test.*, **59**, No.2: 155 (2017).
12. T. Srinivasa Rao, M. Selvaraj, S. R. Koteswara Rao, and T. Ramakrishna, *Materialwiss. Werkstofftech.*, **52**: 308 (2021).
13. T. Srinivasa Rao, S. R. Koteswara Rao, and G. Madhusudhan Reddy, *Materialwiss. Werkstofftech.*, **49**: 851 (2018).
14. V. Kiran Kumar, K. V. Durga Rajesh, S. R. Koteswara Rao, T. Ramakrishna, and T. Srinivasa Rao, *Metall. Res. Technol.*, **121**, No. 107: 1 (2024).
15. J. A. Wert, *Scr. Mater.*, **15**, No. 4: 445 (1981).
16. G. W. Lorimer, *Precipitation Processes in Solids* (Eds. K. C. Russell and H. I. Aaronson) (Warrendale, PA: 1978).